Atmospheric Environment 246 (2021) 118144

Contents lists available at ScienceDirect

Atmospheric Environment

journal homepage: http://www.elsevier.com/locate/atmosenv

Spatiotemporal variability and sources of aerosol water-soluble organic nitrogen (WSON), in the Eastern Mediterranean

Maria Tsagkaraki [a], Christina Theodosi [a], Georgios Grivas [b,*], Evanthia Vargiakaki [a], Jean Sciare [c], Chrysanthos Savvides [d], Nikolaos Mihalopoulos [a,b,c,**]

[a] Environmental Chemical Processes Laboratory, Department of Chemistry, University of Crete, 71003, Heraklion Crete, Greece
[b] Institute for Environmental Research and Sustainable Development, National Observatory of Athens, Palaia Penteli, 15236, Athens, Greece
[c] Climate and Atmospheric Research Center, The Cyprus Institute, 2121, Nicosia, Cyprus
[d] Department of Labour Inspection (DLI), Ministry of Labour, Welfare and Social Insurance, 2121, Nicosia, Cyprus

HIGHLIGHTS

- First WSON measurements and PMF source apportionment at urban/rural sites in Cyprus.
- Water-soluble ON/TN ratios circa 20% with small seasonal and inter-site variability.
- Higher WSON during summer at the background site, larger urban increments in winter.
- Regional secondary WSON sources dominant at the background EMEP site (≈60%).
- Notable WSON contribution (35%) of vehicular emissions at the traffic site.

ARTICLE INFO

Keywords:
WSON
Total nitrogen
Source apportionment
PMF
Eastern mediterranean
Cyprus

ABSTRACT

This study aims to characterize the variability and sources of water-soluble organic nitrogen (WSON) in aerosol over Cyprus in the Eastern Mediterranean. Measurements of PM_{10} particles were conducted during the calendar year of 2011 at two sites, located at a roadside location in Nicosia (urban traffic) and in the rural area of Agia Marina Xyliatou (regional background). Filter samples were analyzed for water-soluble total nitrogen (WSTN), nitrate and ammonium, to determine WSON. Additional analyses were performed, for water-soluble organic carbon (WSOC), organic and elemental carbon (OC and EC), major ions and trace metals. Annual mean WSON concentrations of 0.20 and 0.16 μgN m^{-3} were determined at the urban traffic and regional background sites, respectively. The organic fraction of WSTN was about 20%, with limited inter-site and seasonal variability. Distinct seasonal patterns were observed at the two sites, with warm-period concentrations being significantly higher at the regional background site, while the enhanced local emissions during winter at the traffic site smoothed out the observed variability. Mean WSON/WSOC ratios of 0.09–0.12 were calculated at the two sites, with the two parameters being weakly correlated. A roadside WSON enhancement was verified, although moderate on an annual basis (9%). However, concentrations in Nicosia were more than one time higher than the background during winter. The observed temporal and inter-site variability highlighted the necessity of source apportionment, which was performed using Positive Matrix Factorization (PMF) modeling, utilizing the analytical datasets at the two sites. In this way, the estimated contribution of regional transport of processed aerosols was found to be more pronounced at the regional background site (59% vs. 38%), while a sizeable input (35%) was linked to vehicular emissions at the traffic site. An additional anthropogenic impact, probably related to biomass burning, was estimated at both sites (16%), while contributions of natural sources like mineral dust (4–8%) and marine aerosol (2–3%) were smaller.

* Corresponding author.
** Corresponding author. Institute for Environmental Research and Sustainable Development, National Observatory of Athens, Palaia Penteli, 15236, Athens, Greece.
E-mail addresses: ggrivas@noa.gr (G. Grivas), nmihalo@noa.gr (N. Mihalopoulos).

https://doi.org/10.1016/j.atmosenv.2020.118144
Received 4 June 2020; Received in revised form 30 November 2020; Accepted 10 December 2020
Available online 15 December 2020
1352-2310/© 2020 Elsevier Ltd. All rights reserved.

1. Introduction

Nitrogen compounds are generally recognized as key components of atmospheric aerosol (Duce et al., 1991; Galloway et al., 2003). Their availability in ambient and deposited particles drives aerosol impacts in various aspects, ranging from ecosystem productivity and climate forcing to air quality and health effects (Fowler et al., 2015). From studies on the budget, characteristics and impacts of atmospheric nitrogen, the Eastern Mediterranean has emerged as a focal region. As an ultra-oligotrophic, low-nutrient, low-chlorophyll marine ecosystem with limited riverine inflows, the nutrient input is disproportionally affected by atmospheric deposition (Guerzoni et al., 1999; Krom et al., 2004). The relative abundance of nitrogen in atmospheric aerosol leads to phosphorus-limited productivity characterized by anomalously high N/P molar ratios (Markaki et al., 2010).

The sources and processing of inorganic nitrogen (IN) compounds in aerosols have been studied early on and are well characterized (Russell et al., 1983). However, this is not the case for organic nitrogen (ON) aerosols, although they have been reported to comprise a notable fraction of total aerosol nitrogen at various locations worldwide (Cape et al., 2011). As with any fraction of organic aerosol (OA), the study of organic nitrogen in the particle phase is highly complex. The diversity of its primary sources, gaseous precursors and multiphase chemistry lead to a large number of ON products. These include, inter alia, urea and primary reduced N-compounds, such as amines, amino-acids and peptides, as well as oxidized forms like organo-nitrates (Cornell et al., 2011). Nitrogen-containing aromatic structures, like nitro-PAHS (polycyclic aromatic compounds) and nitro-phenols are of particular importance, due to their enhanced toxic, carcinogenic and mutagenic potential (Harrison et al., 2005; Özel et al., 2010).

Since a substantial portion of bioavailable ON compounds is water-soluble (Fowler et al., 2015), the analytical determination of water-soluble organic nitrogen (WSON) concentrations in aqueous solutions is most frequently used in ON studies (Cornell et al., 2003; Jickells et al., 2013). Highly bioavailable WSON can significantly inflate the previously considered amounts of deposited nitrogen and further impact marine biogeochemical cycling (Matsumoto et al., 2018). In the atmosphere, certain WSON compounds can contribute to new particle formation and growth, through the participation in ternary nucleation and heterogeneous reactions (Qiu and Zhang, 2012; Debevec et al., 2018). Species such as free amino acids of marine biogenic origin, can promote the activation and growth of cloud droplets, thus being implicated in climate forcing (Li et al., 2013). Moreover, certain secondary and humic-like ON substances are light-absorbing and are categorized in brown carbon, wielding an additional effect in the radiative budget (Booyens et al., 2019).

Due to the multitude of effects exerted on ecosystems and the climate, a large part of the research on organic nitrogen aerosols has been focused on remote areas that are representative of concentration levels and processes on regional scales (Cornell et al., 2001; Mace et al., 2003a; Miyazaki et al., 2011). In the Eastern Mediterranean, the properties of organic nitrogen, both in the aerosol phase and in wet deposition, have been examined at coastal regional background sites on Crete, Greece (Violaki and Mihalopoulos 2010; Violaki et al., 2010) and in Southern Turkey (Mace et al., 2003b). Results have highlighted the combined influence of marine aerosols and transported dust, but also of combustion-sources on a regional level. However, several studies conducted in cities around the world have also illustrated an important input from urban sources (Duan et al., 2009; Rastogi et al., 2011), highlighting the need to apportion local vs. regional contributions.

Chen and Chen (2010) were among the first to attempt source identification for WSON, at a coastal site in Taiwan using factor analysis, while more refined results were made available through the application of positive matrix factorization (PMF) modeling (Chen et al., 2010). Yu et al. (2017) explored for the first time the spatial variation of quantified WSON sources across a densely populated metropolitan region (Guangzhou, Pearl River Delta). They reported important contributions from less-frequently considered anthropogenic WSON sources, such as oil combustion emissions and biomass burning (BB). Receptor modeling was also implemented by Liu et al. (2019) in Beijing, to quantify WSON source contributions and highlight their link with the inflammatory potential of fine particles.

In the Eastern Mediterranean area, Nehir and Koçak (2018) applied PMF modeling on a dataset of water-soluble ion concentrations to assess WSON sources in PM_{10} at a coastal site (Erdemli, Southern Turkey). Their results indicated a prevalence of anthropogenic sources, both regional and local. Overall, aerosol sources in this particular region – the Levantine basin – have not been fully characterized. The few results currently available in Cyprus have demonstrated that while air quality can be heavily aggravated during long-range dust transport episodes (Middleton et al., 2008; Achilleos et al., 2014), notable contributions to aerosol formation from local sources – both anthropogenic and biogenic – should be anticipated (Debevec et al., 2017; Pikridas et al., 2018).

In this work, we present experimental results obtained in Cyprus over a 1-year period, where daily-collected PM_{10} filter samples were analyzed to determine WSON concentrations. Measurements were conducted at two sites of contrasting typology (urban traffic and regional background, respectively), allowing for the assessment of the urban roadside enhancement in observed concentrations. Filters were additionally analyzed for an array of chemical constituents and tracers, permitting a thorough characterization of their associations with organic nitrogen. The large analytical dataset was utilized in a receptor modeling framework using PMF analysis, in order to apportion the main aerosol sources and estimate their respective contributions to WSON concentrations at the two sites. To our knowledge this is the first effort in Europe to quantify the spatial and temporal variability of WSON sources, using data from yearlong measurements simultaneously conducted at contrasting sites that are impacted by either long-range transport or urban traffic emissions.

2. Methodology

2.1. Study area and sampling sites

Cyprus is the third largest island in the Mediterranean, lying in the northern Levantine Basin (Fig. 1). The climate type in Cyprus is Mediterranean/Semi-arid, with long dry summers (May–September) and mild wet winters. Peak summer temperatures inland typically exceed 40 °C, while temperature levels rarely fall below zero during winter. Under the influence of cyclonic activity centers in the Mediterranean region, winds flow mainly from SW-W directions during the cold season (Maheras et al., 2004). In the stable conditions of the dry period, while seasonal synoptic-scale winds from N-NW directions prevail, the effect of mesoscale circulations becomes more pronounced, driven by the large surface temperature gradients. Local topography also plays an important role, with circulations being constrained by two mountain ranges, Troodos (1952 m) and Kyrenia (1024 m), in the central and northern parts of the island, respectively. In the area between – the Mesaoria plain – prevailing winds in the W-E axis are occasionally intensified due to funneling effects (Pashardes and Christofides, 1995). Regarding the geographic origin of long-range transported pollution over Cyprus, the long-term (1997–2015) source-region analysis of Pikridas et al. (2018) has established the prevalence of polluted air masses from the northern sector (mainly Turkey and Eastern Europe, with a mean annual frequency of 68%), over air masses associated with dust transport from the southern sector (North Africa and Middle East, 19%) and clean marine air masses from the west (Mediterranean, 8%).

Nicosia, the capital of the Republic of Cyprus and the most populous city on the island (ca. 320,000), is found in the central part of the Mesaoria plain. The city experiences the typical increased traffic conditions of a metropolitan area, albeit with a relatively low circulation of heavy commercial vehicles. Although detailed emission inventories for

residential heating in the area are not available, both heating oil and firewood are known to be used (Georgiou et al., 2020). There are no significantly large point sources in the urban area, with the major industrial installations on the island (3 oil-fired power plants, 2 cement works) situated on the southern coast (at a distance of 40–50 km to the S-SE of Nicosia).

Field measurements were conducted at two sites (indicated in Fig. 1). The first (NIC-TRA), a roadside traffic site (35.1519N, 33.3478E, 176 a.s.l.), was located in the area of Strovolos in Nicosia, at a distance of 10 m from a primary road with dense traffic and frequent congestion during rush hours. NIC-TRA, as part of the regulatory air quality monitoring network in Cyprus, was the site reporting the highest PM_{10} levels during the year leading up to the study period and has continuously recorded mean annual concentrations exceeding the EU annual limit value of 40 $\mu g\ m^{-3}$, between 1998 and 2010 (Pikridas et al., 2018).

The second site (Cyprus Atmospheric Observatory - CAO) is located near (1 km) the village of Agia Marina Xyliatou. This regional background site (35.0380N, 33.0578E, 532 a.s.l.) is placed on a foothill of Troodos mountain, in an area surrounded by shrubland and coniferous forests. Local anthropogenic emissions in the direct vicinity of the site are minimal (Debevec et al., 2018). The site is part of the Global Atmospheric Watch (GAW) and the ACTRIS research infrastructure, and is integrated in the network of the Co-operative programme for monitoring and evaluation of the long-range transmission of air pollutants in Europe (EMEP, name by which the site will be henceforth referred as). The inter-site distance is 28 km and the area between the two sites is characterized by agricultural activity (mainly cereal and feedstock cultivation) and several livestock production plants.

Summary data regarding the meteorological parameters (wind speed, temperature, precipitation) during 2011 in the area of measurements are provided in Table S1. Wind-rose frequency plots are presented for the two sites in Figure S1a. Wind speeds are notably higher on average at the EMEP site, with strong winds not only from the W-NW sectors, as it is common in the area, but also from eastern directions. Conversely, the NIC-TRA site was characterized by low-wind conditions. Pollution roses displaying frequencies of binned PM_{10} hourly concentrations (TEOM) are shown in Figure S1b. Both sites present the highest PM_{10} levels under winds traversing the Mesaoria plain from the west.

2.2. Sample collection and preparation

At the EMEP (regional background) site, PM_{10} aerosol samples were collected on Quartz-fiber filters (150 mm diameter, Whatman, Merck KGaA, Darmstadt, Germany) with a reference-equivalent (CEN 12341) high-volume aerosol collection system (Digitel model DHA-80, Digitel Elektronik AG, Volketswil, Switzerland), sampling at a rate of 30 $m^3\ h^{-1}$. At the NIC-TRA (Nicosia traffic) site, PM_{10} aerosol samples were also collected on Quartz fiber filters (47 mm diameter, Macherey-Nagel GmbH & Co. KG, Dueren, Germany), again using a reference-equivalent sequential sampler (Leckel model SEQ 47/50, Sven Leckel GmbH, Berlin, Germany), at a low-volume flow rate of 2.3 $m^3\ h^{-1}$. A high degree of comparability for measurements between the two types of reference-equivalent samplers (low volume Leckel and high volume Digitel) has been reported for sites in Cyprus (Pikridas et al., 2018).

Quartz filters were pre-combusted at 550 °C for 6 h, to minimize contamination by organic substances. They were weighted pre- and post-sampling with an analytical microbalance (model XP26C, Mettler Toledo LLC, Columbus, OH, USA), following equilibration in stable temperature (20 ± 1 °C) and humidity (50 ± 5%) conditions specified by the CEN 12341 protocol (Pikridas et al., 2018). Next, they were shipped to the University of Crete (Laboratory of Environmental Chemical Processes, Department of Chemistry) for chemical analysis, where they were stored at 4 °C and analyzed within the following two months.

PM_{10} samples were acquired on a daily basis (24-hr, midnight to midnight) over an entire calendar year (January to December 2011). At EMEP, 339 PM_{10} samples were sampled, of which 129 were analyzed for water-soluble total nitrogen (WSTN), with the respective numbers at NIC-TRA being 358 and 189. The number of same-day samples from the two sites analyzed for WSTN was 88, evenly distributed around the year. Blank filter samples were also collected and analyzed following exactly the same procedures. They were used to perform blank corrections for all quantified components and also for the determination of the uncertainties used as input in the source apportionment analysis.

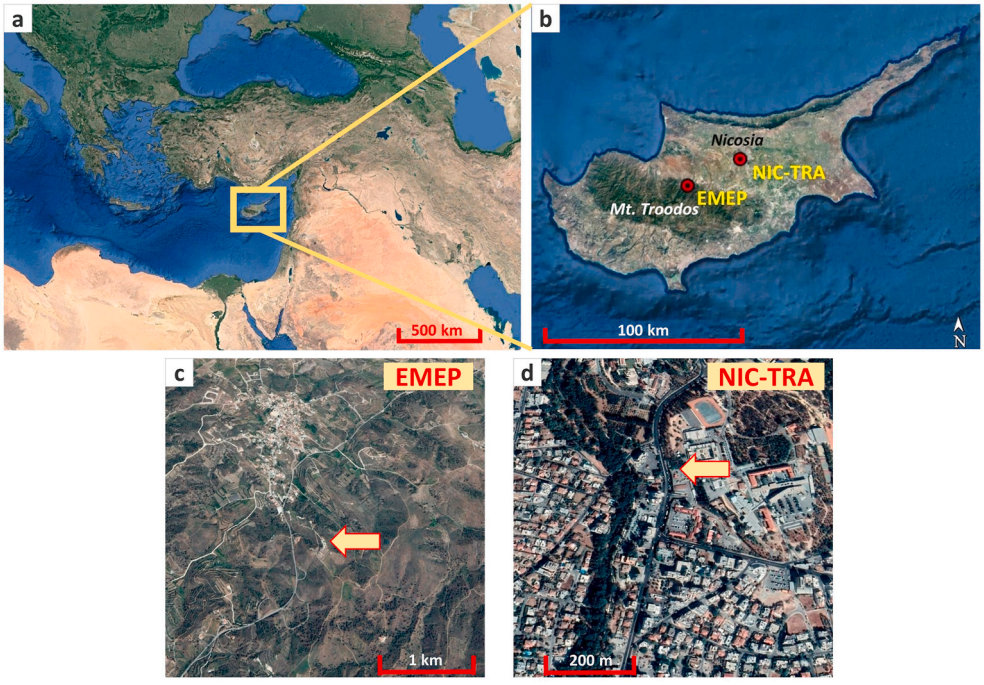

Fig. 1. Geographical location of Cyprus in the Eastern Mediterranean region (a,b) and of the two samplings sites in Cyprus: EMEP (regional background site in Agia Marina Xyliatou) and NIC-TRA (urban traffic site in Nicosia). Close overviews of the two sites are presented in the two lower panels (c: EMEP, d: NIC-TRA).

2.3. Chemical analysis

To determine the concentrations of water-soluble total nitrogen (WSTN), water soluble organic carbon (WSOC) and major water-soluble ionic species (including NO_3^- and NH_4^+, which were required for WSON calculations), part of the filter sample was extracted in an ultrasonic bath, for 45 min in 20 ml of ultra-pure grade water (18.2 MΩ). Before the analysis for water-soluble species, the extracts were filtered using syringe filters (0.45 μm pore size).

A Total Organic Carbon analyzer (TOC-V_{CSH} Analyzer, Shimadzu Corporation, Kyoto, Japan) coupled with a Total Nitrogen module (TNM-1, Shimadzu Corporation) was used to determine WSTN as well as WSOC concentrations. The operating principle for TN measurements is based on catalytic combustion-oxidation (Pt catalyst, 720 °C), followed by chemilluminescence detection of NO produced from the decomposition of nitrogen compounds (Miyazaki et al., 2014; Chen et al., 2018).

The carrier gas (high-purity dry air) first sweeps CO_2, produced in the combustion tube during the oxidation step, into a non-dispersive infrared detector (NDIR), where water-soluble total carbon (TC) is quantified. Inorganic carbon (mainly carbonate carbon) contained in the aqueous solution is also measured at the detector following acidification and sparging of CO_2, and is subtracted from water-soluble TC to obtain WSOC concentrations. For the total nitrogen (TN) quantification, the stream is carried to the nitrogen module, where it is mixed with ozone. Its reaction with NO generates NO_2 molecules at an excited state (NO_2*). The excess energy, emitted as light when NO_2* relaxes to its ground state, is measured by a chemilluminescence detector with a photomultiplier tube.

WSON was calculated as the difference between WSTN and the total nitrogen contained in inorganic species (NO_3^- and NH_4^+) which were determined by ion chromatography (IC). Concentrations of nitrite ions (NO_2^-) have been invariably found below ion chromatography detection limits and were not considered further in the present study. Negative WSON concentrations (6.2% and 7.4% of samples at EMEP and NIC-TRA, respectively) were included in mean value calculations as zero (Mace et al., 2003b; Violaki and Mihalopoulos, 2010). Standard solutions were prepared using high purity (≥99.5%, Fluka, Honeywell International Inc., Charlotte, NC, USA) reagents (KNO_3, potassium hydrogen phthalate and Na_2CO_3/$NaHCO_3$).

Ion chromatography (IC) analysis was applied to determine the concentrations of water-soluble inorganic nitrogen (WSIN) ions (NO_3^-, NH_4^+) and other major ionic species (Cl^-, Br^-, NO_3^-, HPO_4^{2-}, SO_4^{2-}, $C_2O_4^{2-}$, Na^+, NH_4^+, K^+, Mg^{2+} and Ca^{2+}). A Dionex DX-500 system (Thermo Fisher Scientific Inc., Waltham, MA, USA) was used, with an AS4A-SC column and an ASRS-I suppressor operating in auto-suppression mode for anions, and a CS12-SC column with a CSRS-I suppressor for cations (Bardouki et al., 2003; Paraskevopoulou et al., 2014).

In addition to water-soluble species, samples were analyzed for organic carbon (OC), elemental carbon (EC) and elemental (trace metal) composition. Concentrations of OC and EC were determined by thermal-optical analysis, according to the EUSAAR-2 protocol (Cavalli et al., 2010), using a Sunset analyzer (Sunset Laboratory Inc., Portland, OR, USA). Concentrations of the secondary OC component (SOC) at EMEP were estimated using the EC-tracer method (Turpin and Huntzicker, 1995), with the season-specific 5% lowest percentile of measured OC/EC ratios, selected as the primary OC/EC ratios (Kaskaoutis et al., 2020). Concentrations of major (Al, Ca, Fe) and trace (Ti, V, Cr, Mn, Ni, Cu, Zn, As, Cd, Pb) elements were determined using inductively-coupled plasma mass spectrometry (ICP-MS, NexION 300X, PerkinElmer Inc., Waltham, MA, USA), following acid microwave digestion (Theodosi et al., 2010).

2.4. WSON source identification and apportionment

Positive Matrix Factorization (PMF) analysis (Paatero and Tapper, 1994), using the chemical speciation dataset, was applied for the identification and apportionment of WSON sources at the two sites. Although the PMF approach is regularly followed for the attribution of sources to total aerosol mass, as a weighted regression scheme it has been similarly utilized for the apportionment of identified source contributions to specific aerosol components as well (e.g. organic and black carbon) [Briggs et al., 2016; Srivastava et al., 2018]. PMF analysis on chemically speciated data for WSON source apportionment has only recently been implemented, with results being reported by Chen et al. (2010), Yu et al. (2017), Nehir and Koçak al (2018). and Liu et al. (2019).

Positive matrix factorization was applied on a dataset of 18 aerosol components, including OC, EC and selected ions and trace elements. The EPA PMF 5.0 software (Norris et al., 2014), based on the multilinear engine (ME-2) program (Paatero et al., 1999) was used. A total of 101 and 119 (24-h integrated) samples where WSON has been determined along with all other aerosol components were included in the PMF analysis for EMEP and NIC-TRA, respectively. Samples for which at least one type of analysis (OC/EC, IC, ICP) was missing were excluded from the PMF dataset. Samples with negative WSON values (less than 7% of analyzed samples) were also excluded. Given the contrasting site types, separate PMF models were run for each one. Multiple runs with a varying number of factors were performed while monitoring the changes in the ratio Q/Q_{exp} of observed/expected values of the Q objective function (small decreases in the ratio by increasing number of factors is an indication of redundancy) [Comero et al., 2009]. Information on the Q/Q_{exp} trends for models with different number of factors are presented in Table S2. Only solutions with factors for which a meaningful physical characterization was feasible were retained.

The general PMF methodological approach followed here is described in more detail in Grivas et al. (2018) and Theodosi et al. (2018). In brief, uncertainties were calculated based on analytical detection limits and precision for aerosol components (Norris et al., 2008). Data points with concentrations below detection limits were substituted by one half of the detection limit and were assigned 5/6 of the respective detection limit as uncertainty (Polissar et al., 1998). For WSON, since it is calculated as the difference of total WSTN and WSIN, its uncertainty was propagated (Nehir and Koçak, 2018; Grivas et al., 2018) from the respective calculated uncertainties (as the square root of the sum of squared uncertainties). The selection of species for the PMF analysis was based on the signal-to-noise (S/N) ratio (Paatero and Hopke, 2003). Species for which the S/N ratio was smaller than 0.5 were excluded from the PMF analysis, while those with ratios between 0.5 and 2 had their uncertainty tripled (Table S2). WSOC and oxalate as well as Ca^{2+} were also excluded, to avoid double counting with OC and elemental Ca, respectively (Reff et al., 2007). A value of 12% was selected as additional modeling uncertainty to encompass unaccounted errors and variations in source profiles, leading to more stable solutions (Hasheminassab et al., 2014). Rotational ambiguity and random errors were assessed using the displacement (DISP) and bootstrap (BS) procedures, respectively, which are embedded in the EPA PMF software (Paatero et al., 2014). The specific model parameters and diagnostics for the selected solutions at the two sites are presented in Table S2, according to the reporting guidelines presented by Brown et al. (2015).

2.5. Ancillary data and data analysis

The distributions of all analytical data were tested for normality (Shapiro-Wilk test), to decide upon the use of parametric (t-tests, paired t-tests, ANOVA) or non-parametric (Mann-Whitney, Wilcoxon, Kruskal-Wallis) tests, in order to evaluate the statistical significance (p) of differences between independent samples, paired samples and multiple groups, respectively. Auxiliary data on concentrations of regulated pollutants (NO_x, CO, O_3, SO_2, PM_{10}, $PM_{2.5}$) and of meteorological parameters were used at the two sites, to characterize the factors controlling the temporal variability of WSON and validate externally the identified sources. For the assessment of long-range influences on

concentrations and source contributions, five-day back trajectories, arriving at the EMEP site every 12-h, were obtained using the Hybrid Single Particle Lagrangian Integrated Trajectory model (HYSPLIT). Consequently, the airflows to Cyprus, were classified by trajectory analysis in 7 classes, based on their apparent source region (Kouvarakis et al., 2000; Kleanthous et al., 2014; Debevec et al., 2017). To study the effects of ground-level circulation on smaller spatial scales, bivariate (wind speed-direction) polar plots for concentrations and conditional probability functions (CPF) were constructed, as described by Uria--Tellaetxe and Carslaw (2014), using the OpenAir package of the R software.

3. Results and discussion

3.1. Characterization of WSON concentrations

Descriptive statistics for WSON and other WSTN components (NO_3^-, NH_4^+) in PM_{10} particles, sampled during the year of measurements (2011) at the two sites, are presented in Table 1. Concentrations of WSON are expressed in units of μgN m^{-3}, throughout the text. A detailed comparison of mean observed WSON levels (and their contributions to WSTN) with the recent literature is provided in Table S3.

The annual mean concentration of WSON at EMEP was 0.16 ± 0.13 μgN m^{-3}, with a daily maximum of 0.52 μgN m^{-3}. The mean value is close – although somewhat lower – to those observed in PM_{10} at coastal regional background sites in the Eastern Mediterranean. At the Finokalia site on the island of Crete, Violaki and Mihalopoulos (2010) reported mean WSON concentrations of 0.24 μgN m^{-3} during 2005–2006, while Nehir and Koçak (2018) at the Erdemli site in Southern Turkey recorded a higher annual mean of 0.33 μgN m^{-3} in 2014–2015. It appears that background WSON concentrations may exhibit considerable spatial variability within the same region (as in the present case for the Eastern Mediterranean). Although inter-annual differences cannot be excluded here, the comparison between studies in Southern Turkey (Erdemli) conducted 15 years apart (Mace et al., 2003b; Nehir and Koçak, 2018) did not produce important differences (spring averages of 0.41 μgN m^{-3} in 2000 and 0.39 μgN m^{-3} in 2014–2015). A potential factor leading to lower WSON concentrations in Cyprus might be the unusually low frequency and intensity of dust transport during the year of measurements (only one day with PM_{10} exceeding 150 μg m^{-3} at EMEP), with a lack of the usually very intense summer dust episodes (Middleton et al., 2008; Pikridas et al., 2018). Nevertheless, the regional background of WSON in the Eastern Mediterranean remains much higher (from two-fold to one order of magnitude) than at remote insular locations in the Atlantic and Indian Oceans (Violaki et al., 2015; Altieri et al., 2016), highlighting the major contribution of continental against marine emissions.

Moderately higher WSON concentrations were observed at the urban traffic site (NIC-TRA), with an annual mean of 0.20 ± 0.14 μgN m^{-3}, although the upper range (daily maximum of 0.56 μgN m^{-3}) was comparable to that observed at EMEP, implying that roadside conditions were not sufficient to induce extreme WSON levels. Overall, WSON levels measured in Nicosia were comparable to those reported by long-term studies in urban areas of the United States and Japan, but considerably lower than levels observed in polluted Chinese megacities, where long-term average WSON concentrations up to several μgN m^{-3} have been documented (Wang et al., 2013; Ho et al., 2015; Chen et al., 2019), mostly due to massive anthropogenic emissions on both regional and local levels. Generally, studies presenting WSON measurements at roadside locations remain scarce, while the urban vs. regional background relationships have not been well characterized so far. Rastogi et al. (2011) reported urban levels comparable to NIC-TRA, at a downtown site in Atlanta and a similar absence of a significant urban enhancement compared with a rural-background site. Results for an urban vs. forested site-pair in the Yamanashi Prefecture, Japan (Matsumoto et al., 2014), showed urban levels similar to NIC-TRA, but with a larger urban increment. Other studies have also reported limited urban vs. rural background contrasts (e.g. Montero-Martinez et al., 2014, in the area of Emilia Romagna, Italy) or even higher levels at rural sites close to large urban agglomerations (Yu et al., 2017, in the Pearl River Delta, China).

Organic compounds accounted for about one-fifth of WSTN at both sites (18% at EMEP and 19% at NIC-TRA), with WSON/WSTN displaying moderate variability (the 95° percentile of the ratio at both sites was below 0.4). The monthly concentration patterns of WSTN and its components are displayed in Fig. S2, with the WSON/WSTN contributions being fairly stable among seasons at both sites (mean seasonal ratios ranging between 16 and 24%). The mean WSON contribution (%) calculated at EMEP was between those reported at regional background sites in Crete (13%; Violaki and Mihalopoulos, 2010) and in the Mersin province, Turkey (29%; Nehir and Koçak, 2018). Mean WSON/WSTN fractions in the order of 20% and small urban vs. regional contrasts have also been reported in areas like Bologna, Italy and Kofu, Japan (Matsumoto et al., 2014; Montero-Martinez et al., 2014), although a wide range of WSON/WSTN (10–45%) mean ratios has been documented at various urban sites for $PM_{2.5}$ samples (e.g. Rastogi et al., 2011; Ho et al., 2015). The results indicate that ON is an important component of the nitrogen cycle throughout the year in the Eastern Mediterranean, suggesting the benefits from its incorporation in relevant atmospheric chemistry-transport and deposition models (Kanakidou et al., 2020).

The WSON component drives a substantial amount of WSTN variability (21–43%), as inferred by the coefficients of determination in Fig. S3. It is, however, weakly correlated with its ionic nitrogenous counterparts (probably with the exception of ammonium at EMEP). The ammonium ion, mainly through its participation in the regionally transported ammonium sulfate appears to control total aerosol nitrogen (r^2: 0.72, 0.78, at NIC-TRA and EMEP, respectively) [Bardouki et al., 2003; Sciare et al., 2008]. On the other hand, while comprising large fractions of WSTN (33–43%), nitrate was not strongly correlated with WSTN (r^2: 0.09, 0.34 at NIC-TRA and EMEP, respectively). In general, such daily correlation patterns, have been reported by other studies, indicating not only the diversity of WSON emissions but also their changing intensity and evolution on seasonal and diurnal scales (Rastogi et al., 2011; Matsumoto et al., 2014).

The mean WSON/WSOC mass ratio was calculated at 0.12 ± 0.09 and 0.09 ± 0.06 at EMEP and NIC-TRA, respectively, with maximum

Table 1
Nitrogen species in PM_{10} aerosol samples collected at two sites in Cyprus (EMEP and NIC-TRA), from January to December 2011: Statistical summary of water-soluble organic nitrogen (WSON), NO_3^- - N, NH_4^+ - N and water-soluble total nitrogen (WSTN) concentrations (μgN m^{-3}).

EMEP (Agia Marina Xyliatou), number of samples: 129				
	WSON	NO_3^- - N	NH_4^+ - N	WSTN
Arithmetic mean (standard error)	0.16 (0.01)	0.30 (0.02)	0.45 (0.02)	0.91 (0.04)
Standard deviation	0.13	0.19	0.25	0.41
Median	0.13	0.25	0.42	0.88
Range	0.00–0.52	0.02–1.23	0.02–0.95	0.14–1.95
Interquartile range	0.07–0.23	0.18–0.39	0.25–0.63	0.58–1.22
10° – 90°	0.03–0.35	0.12–0.53	0.10–0.84	0.40–1.53
Relative contribution to WSTN (%)	18	33	49	
NIC-TRA (Nicosia), number of samples: 189				
	WSON	NO_3^--N	NH_4^+ - N	WSTN
Arithmetic mean (standard error)	0.20 (0.01)	0.46 (0.02)	0.40 (0.02)	1.05 (0.03)
Standard deviation	0.14	0.21	0.31	0.38
Median	0.17	0.41	0.35	0.99
Range	0.00–0.56	0.10–1.29	0.01–1.42	0.37–2.27
Interquartile range	0.10–0.28	0.33–0.54	0.19–0.54	0.79–1.27
10° – 90°	0.01–0.38	0.23–0.87	0.06–0.87	0.61–1.57
Relative contribution to WSTN (%)	19	43	38	

daily values not exceeding 0.40. The mean values are in the range of N:C ratios in organic aerosols that is typically reported by relevant studies (e.g. Yu et al., 2017) and with the same urban-to-regional increasing pattern. Although it is difficult to characterize chemically the WSON compounds based on ON/OC ratios, these results certainly indicate an important continental enrichment against marine background aerosols (Facchini et al., 2008). The seasonal variability of the WSON/WSOC ratio at NIC-TRA was not statistically significant ($p = 0.06$), however, at the regional background site the mean ratios were significantly higher during spring and summer ($p < 0.01$). A similar seasonal pattern was reported by Chen et al. (2018) in the forested environment of the Appalachian Mountains, where the spring-summer increase has been attributed to increased biogenic emissions combined with secondary aerosols. It is interesting that this increase at EMEP came in parallel with the significant warm-period (May–October) increase of WSOC concentrations, indicating that secondary processing could enhance the inclusion of nitrogen in secondary organic aerosols (Montero-Martinez et al., 2014; Yu et al., 2017).

WSON and WSOC were not outright correlated on an annual basis ($r = 0.37$, at both sites), indicating differences in the relative importance of sources and their seasonal dependence (Chen et al., 2018). The water-soluble OC component was dominant (comprising 58% and 80% of OC, at the urban and background sites, respectively), mostly indicating the importance of secondary aerosol processing (Sciare et al., 2008; Paraskevopoulou et al., 2014). In view of this, the weak overall WSON–WSOC association suggests the additional contribution from primary and less-aged ON emissions.

3.2. Temporal variability of WSON and controlling factors

The seasonal variation of mean WSON concentrations at the two sites is displayed in Fig. 2, while a breakdown of levels by air mass sector is provided in Table S4. At the regional background site, the seasonal variability was statistically significant ($p < 0.01$), with the mean concentration in summer (0.29 μgN m^{-3}) being notably higher than in winter (0.10 μgN m^{-3}) and in the two transition seasons (0.14 μgN m^{-3}). The summer period was dominated by air masses from the northern sector (with a 93% frequency), which transport processed organic aerosols deriving from combustion and biogenic emissions in Turkey and Eastern Europe (Lelieveld et al., 2002; Sciare et al., 2008). Air masses from the northern sector were also frequent during the rest of the year (65%), however, aerosol rainout and scavenging in the wet period should be effective mechanisms for removal of soluble ON compounds (Altieri et al., 2016). While during summer there was virtually no rainfall (0.7 mm in total) in the vicinity of EMEP, the mean WSON concentration during days with rainfall in the other months was significantly decreased (0.09 μgN m^{-3} against 0.18 μgN m^{-3} during clear days, $p < 0.01$).

The importance of large-scale transport and aging mechanisms on WSON levels is also implied by the significant correlations (Table S5) registered with secondary aerosol components like non sea-salt sulfate (nss-SO_4^{2-}) and oxalate (r: 0.58 and 0.42, respectively). The formation of these ions is driven by both heterogeneous and photochemical mechanisms, which promote ON levels as well (Ervens et al., 2011; Jickells et al., 2013). Moreover, WSON was positively associated with the daily maximum temperature ($r = 0.49$) and the daily mean O_3 concentration ($r = 0.38$), as were sulfate and oxalate, suggesting the photochemical formation of ON products during warm conditions, through the reaction of nitrogen oxides and volatile organic compounds (VOCs). At the same site, which is surrounded by vegetation, Debevec et al. (2017) have reported on the local emissions and the temperature dependence of biogenic VOCs, such as isoprene and a-pinene, whose oxidation products have been reported in literature to correlate well with organic nitrogen (Miyazaki et al., 2014).

The enhanced formation of secondary organic nitrogen during the photochemical season is further indicated by the similarities between WSON and OC, WSOC monthly variabilities (Fig. 3). Although statistically significant, year-round correlations (Table S5) of WSON with OC ($r = 0.47$), WSOC ($r = 0.37$) and SOC ($r = 0.55$) were moderate, as it is frequently reported (Rastogi et al., 2011; Matsumoto et al., 2014; Chen et al., 2019). Apart from other regional sources (e.g. dust and marine aerosols), the apparent additional contributions of primary ON particles could be also related to local wind systems prevailing in the area that carry to the site biogenic ON particles from the surrounding woodland (Miyazaki et al., 2014).

The intra-annual profile of WSON at the traffic site in Nicosia was markedly different, since the seasonal variability (Fig. 2) was not found statistically significant ($p = 0.65$), with only a small increase during summer (14%), compared to the other seasons combined. As a result, WSON concentrations at NIC-TRA were higher than at EMEP during all seasons except summer, when urban emissions minimize (Mouzourides et al., 2015) and the regional/photochemical influence is enhanced (see above). As it appears in Fig. 4, WSON levels at the urban location generally track the monthly variability of EC and also of OC, WSOC,

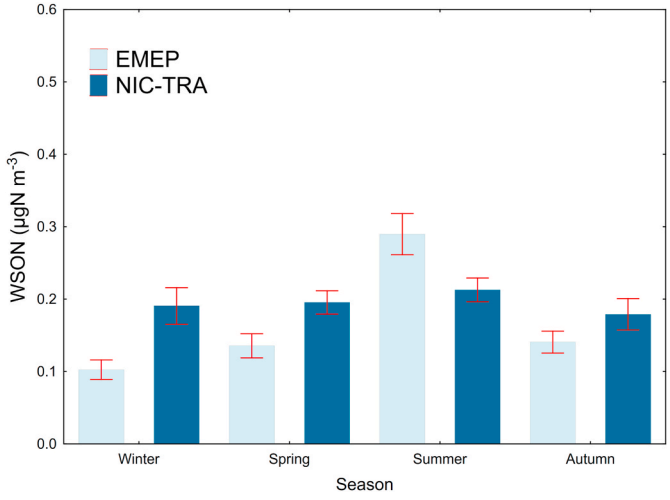

Fig. 2. Seasonal variation of mean (±one standard error of the mean) water-soluble organic nitrogen (WSON) concentrations at the two sites, during the calendar year of 2011.

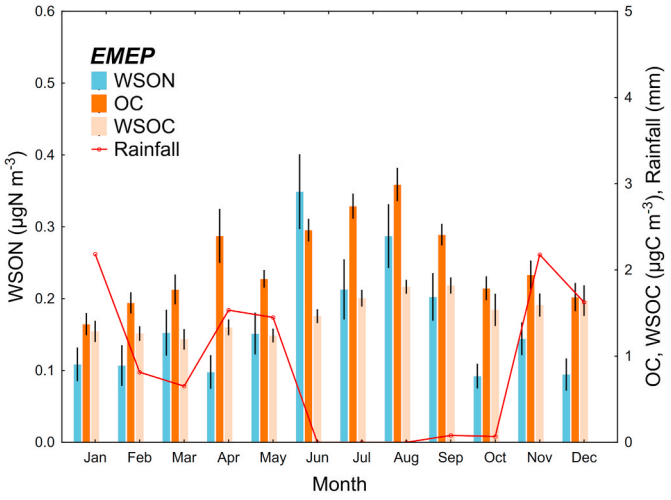

Fig. 3. Monthly variation of mean water-soluble organic nitrogen (WSON) concentrations, in comparison with carbonaceous components (organic carbon – OC, water-soluble organic carbon – WSOC) at the regional background site. Error bars correspond to one standard error of the mean. A line denoting monthly average values of recorded 24-h total rainfall amounts is overlaid.

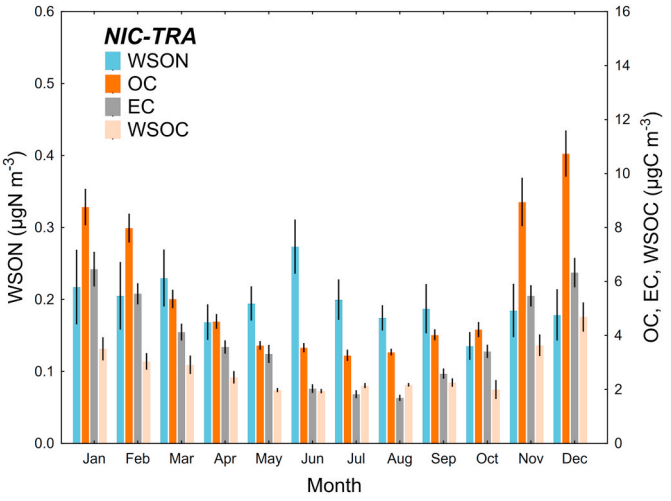

Fig. 4. Monthly variation of mean water-soluble organic nitrogen (WSON) concentrations, in comparison with carbonaceous components (organic carbon – OC, elemental carbon – EC, water-soluble organic carbon – WSOC) at the urban traffic site. Error bars correspond to one standard error of the mean.

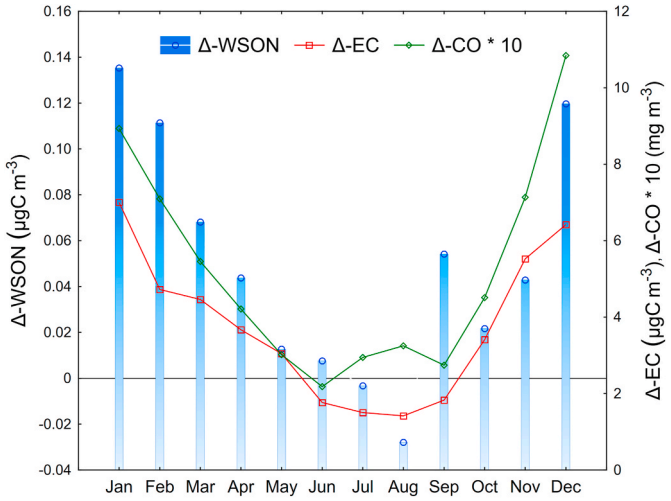

Fig. 5. Monthly variation of the "urban + traffic" enhancement for water-soluble organic nitrogen (Δ-WSON), in comparison with the respective enhancements for traffic-related pollutants: elemental carbon (Δ-EC) and CO (Δ-CO).

during the colder half of the year (November–April). In this period, daily concentrations of WSON at the traffic site co-varied fairly well with indicators of combustion emissions such as the carbonaceous components EC, OC (r = 0.68, 0.66, respectively) and primary gaseous pollutants like NO_x, CO (r = 0.69, 0.68, respectively). Moreover, in this period, mean WSON concentrations were higher (23%) during working days as opposed to weekends when traffic emissions diminish. The indicated substantial cold-period input from urban emissions should also include residential biomass burning as evidenced by the significant cold period correlation (r = 0.51) with K^+ (Ye et al., 2017).

3.3. Inter-site variability and urban enhancements

The mean difference between the two sites during common WSON measurement days was 9% (higher at NIC-TRA). Inter-site differences for pairwise comparisons of WSON concentrations were not statistically significant on an annual basis at the 0.05 level (p = 0.18), although they were significant (p < 0.01) during the cold period, when the average concentration was higher at NIC-TRA by 65%. The overall inter-site correlation for WSON was statistically significant (p < 0.01) but moderate (r = 0.48), further indicating the contrasts between sources at the two sites.

To study the potential enhancement of WSON concentrations at the roadside site, the "Lenschow approach" (Lenschow et al., 2001) was followed, by assuming that WSON at the traffic site is the sum of a "regional" component (WSON measured at the EMEP site) and an "urban + traffic" component, calculated as the concentration difference between NIC-TRA and EMEP (hereafter referred as Δ-WSON). The "urban + traffic" enhancements for other traffic-related particle and gaseous pollutants (Δ-EC, Δ-CO, Δ-NO_x) were likewise calculated. The monthly variability of these enhancements is displayed in Fig. 5, with evident similarities in the seasonal cycles for WSON and the other primary pollutants. High "urban + traffic" contributions were observed in the winter period, along with a large decrease during the summer months. This monthly pattern of "urban + traffic" enhancements (from Agia Marina Xyliatou to Nicosia) has also been observed for PM_{10} and $PM_{2.5}$ in previous studies (Achilleos et al., 2014; Pikridas et al., 2018). Apart from local dispersion dynamics (stagnation at Nicosia in shallow boundary layer conditions during winter), the seasonal difference in the enhancement can be ascribed to the summer reduction of urban emissions, along with increased biogenic emissions from the surrounding forest at the background site. When comparing Δ-WSON with the enhancements for the other traffic-related pollutants on a daily basis, the associations become less obvious (Fig. S4). Nonetheless, the statistically significant correlation coefficients, ranging in 0.5–0.6, provide an indication that the contribution of combustion-related emissions to urban WSON concentrations should be acknowledged. In fact, vehicular exhaust emissions are lately being recognized as a measurable source of ON compounds in urban areas (Yu et al., 2017; Liu et al., 2019).

The analysis of wind effects on observed WSON levels and "urban + traffic" enhancements can provide a broad idea for their local and sub-regional spatial variability and suggest small-scale transport patterns. Bivariate polar plots, which associate wind direction and speed with WSON concentrations at NIC-TRA and EMEP, are presented in Fig. 6a and b. Higher WSON levels can be seen (especially at NIC-TRA) under stronger-than-average winds from the western sector, which channel polluted continental air masses through the entrance of the Mesaoria plain (Pashardes and Christofides, 1995). This westerly incremental effect has been observed also for PM_{10} particles in Nicosia (Mouzourides et al., 2015). Moreover, low-wind conditions appear to favor the accumulation of locally produced WSON at NIC-TRA (where plots strongly localized at the center were produced for all traffic pollutants; not shown). At EMEP, in accordance with its regional background character, sectors linked to high WSON concentrations were more widely dispersed, although transport from the north of the site, under favorable wind circulation cannot be ruled out, as it has been demonstrated by Debevec et al. (2017) for VOC emissions. Conversely, the polar plot for Δ-WSON (Fig. 6c), shows an omnidirectional increase around the center at low-to-moderate winds, consistent with the pattern of the respective EC enhancement (Δ-EC, Fig. 6d), which clearly demonstrates the dominant effect of local urban emissions, under low-wind conditions (Grivas et al., 2018; Stavroulas et al., 2019).

3.4. Source apportionment of WSON

The contribution of resolved sources to the aerosol components included in the PMF analysis is displayed in Fig. 7, while the respective fractional contributions of sources to WSON mass are given in Table 2. The monthly variability and CPF plots for contributions of selected sources are provided in supplementary Fig. S6 and Fig. S7, respectively. Detailed information on parameters and performance of selected PMF solutions are gathered in Table S2. The temporal variability of WSON concentrations was adequately reconstructed by models at both sites, with r values of 0.85 and 0.83 at EMEP and NIC-TRA, respectively, and

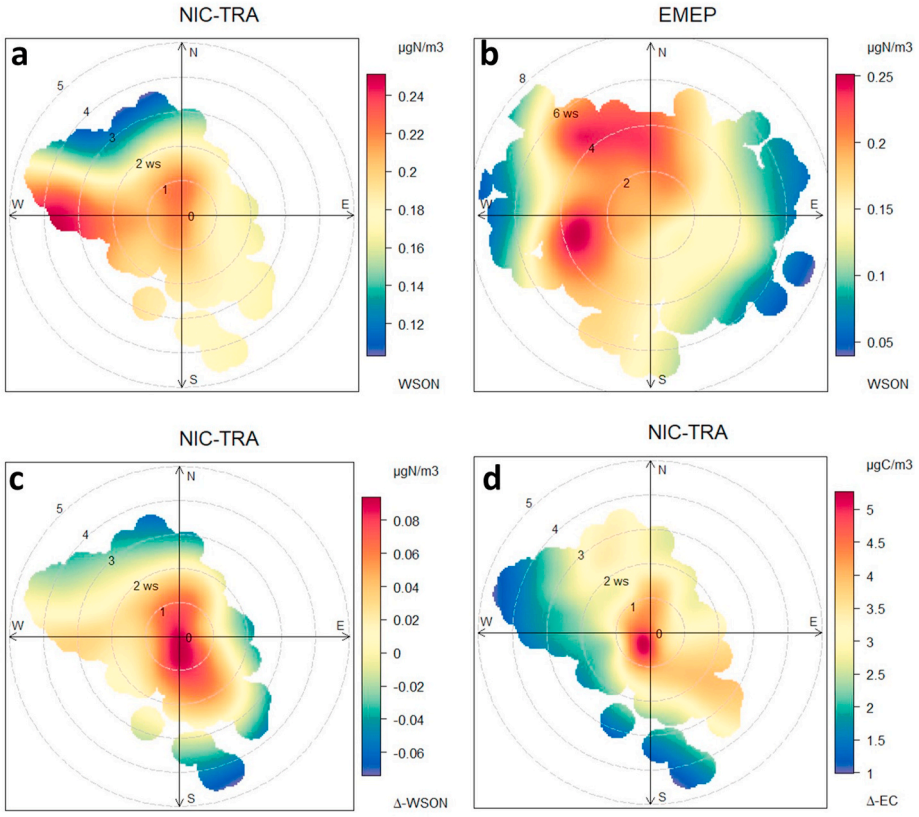

Fig. 6. Bivariate (wind speed, wind direction) polar plots for water-soluble organic nitrogen (WSON) concentrations at NIC-TRA (a) and EMEP (b), and for "urban + traffic" enhancements of WSON (Δ-WSON, c) and elemental carbon (Δ-EC, d). Plots for Δ-WSON, Δ-EC based on wind data as measured at the urban site. All plots calculated from days with concurrent WSON measurements at the two sites. Radial axis (ws: wind speed) in m s^{-1}.

unaccounted mass fractions of approximately 5%.

At both sites, sources related to regional secondary processing, marine aerosol and mineral dust were identified, along with a K-rich factor most likely related to biomass burning. Additionally, at the regional background site, a fossil fuel combustion source was extracted, while at the urban traffic site two sources related to vehicular emissions and traffic-related dust resuspension, respectively, were isolated. The traffic-related dust factor, characterized by the presence of mineral elements together with markers of brake and tire wear (Fe, Cu, Zn, Pb) was not associated with WSON and its contribution profile is included separately, in supplementary Fig. S5. The obtained solutions were robust, as evaluated by the displacement (no factor swaps, very low % dQ change) and bootstrap methods (97–100% and 99–100% of correct factor mapping, at NIC-TRA and EMEP respectively). The base solution obtained for NIC-TRA was rotated using an FPEAK value of −0.4 to achieve a clearer separation between factors in the G-space plots (Paatero et al., 2002). The spatiotemporal variability of each resolved factor and their contribution to WSON is discussed below.

Regional secondary aerosol: This factor is characterized by high contributions to sulfate and ammonium ions. It was identified in both PMF solutions and was well-correlated among sites ($r = 0.70$), apparently being spatially effective over Cyprus, which is consistent with its transboundary character. Trace elements of anthropogenic origin were also associated with the factor. Their long range transport from distant sources along with the processed aerosol mixture, is frequently reported for sites in Southeastern Europe (Grivas et al., 2018). During days with continental air masses arriving from the north (mainly N, NW) there was an 85% increase in the factor contributions, compared with air masses from the southern-western sectors. The source profile was characterized by large OC/EC ratios (up to 9.5 at EMEP), indicating the high degree of atmospheric processing. Moreover, the WSON/OC ratios (up to 0.2 at EMEP) were the highest among sources apportioned at both sites, supporting a link between secondary processing and nitrogen abundance in organic aerosols. The source contributions were significantly enhanced (shown in Fig. S6 for EMEP) during the warm period ($p < 0.05$), similarly to secondary aerosol components (e.g. WSOC). The factor contributed heavily to WSON levels at the background site (59%), while also recording the highest contribution at the urban site (38%). Regionally processed aerosol has been consistently identified as a source in WSON apportionment studies. For the regional background of the Eastern Mediterranean, Nehir and Koçak (2018) have estimated a comparably large (42%) contribution of secondary aerosol sources to WSON for PM_{10}

Marine aerosol: The factor is identified by the presence of chloride, and contributes considerably also to concentrations of the magnesium ion in the source profile. The inter-site correlation was high ($r = 0.87$), indicative of a common source. CPF plots (Fig. S7) for both sites indicate higher contributions from the W-NW sector, where the distance from the northern coast of Cyprus is smaller and stronger inflows are more frequent. The factor's contribution to WSON was very small at both sites (2–3%) and close to the 5% contribution reported by Nehir and Koçak (2018) in Erdemli Southern Turkey, 180 km NW of Nicosia, near the Mediterranean coast. Achilleos et al. (2016) have also found sea-salt contributions of 2% and 11% in fine and coarse PM, respectively, in Nicosia, along with high inter-site correlations over Cyprus. The presence of organic nitrogen in marine aerosols has been mainly linked to reduced N compounds of biological origin. The source apportionment analysis of Chen et al. (2010) reported a strong association of the sea-salt factor with low molecular weight ON compounds (e.g. free amino-acids). Also, in coastal Crete, Violaki and Mihalopoulos (2010) determined a combined contribution of about 3% for free amino acids and methylamine, to WSON measured in PM_1.

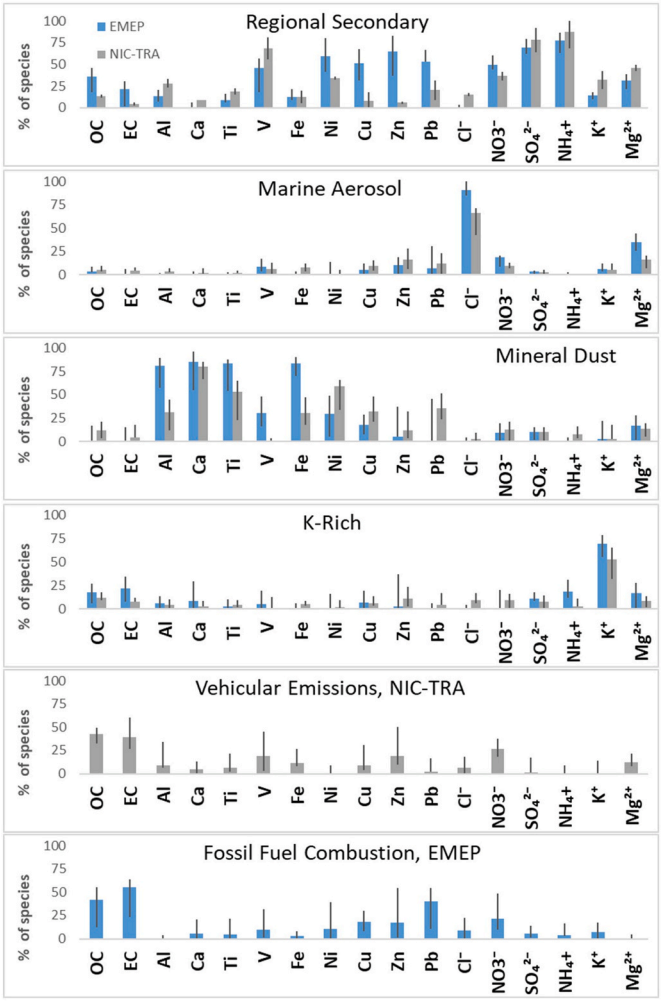

Fig. 7. Explained variance of sources identified by Positive Matrix Factorization Analysis (PMF) at the EMEP (blue bars) and NIC-TRA (grey bars) sites. Error bars for 5° – 95° percentiles from 100 bootstrap resamples. (For interpretation of the references to colour in this figure legend, the reader is referred to the Web version of this article.)

Table 2
Contribution (%) of sources to water-soluble organic nitrogen (WSON) concentrations, as estimated by Positive Matrix Factorization (PMF) analysis, at the two sites. Pearson correlation coefficients for inter-site comparisons of contributions are also provided, for factors of common characterization.

	EMEP	NIC-TRA	Inter-site correlation
	(% of WSON)	(% of WSON)	
Regional secondary	59.3	38.2	0.70*
Marine aerosol	2.9	2.3	0.87*
Mineral Dust	9.4	3.8	−0.18
K-rich	16.5	15.8	0.25
Vehicular emissions	–	35.0	–
Fossil fuel combustion	6.4	–	–
Unaccounted	*5.5*	*4.9*	

* Significant at the 0.01 level.

Mineral dust: The factor, characterized by high contributions to mineral elements (Al, Ca, Fe, Ti) was determined at both sites. The impact of dust in Cyprus, from local resuspension but also due to outbreaks of transported dust, has been extensively documented (e.g. Achilleos et al., 2014). Moreover, increased soil resuspension (Pikridas et al., 2018) during the dry period may combine with the occasional LRT dust intrusions, explaining the observed temporal variability of the factor at the background site (Fig. S6). The comparative assessment of CPF plots (Figure S7) between the two sites supports the possibility for local dust contributions, given the limited impact of LRT dust during the study year. It has to be noted though, that the warm/cold period difference was significant ($p < 0.01$) only at the background site, indicating the more local character of the source in the absence of intense dust transport episodes. The average contribution of the factor to WSON was moderate, lower at the urban (4%) than at the background (9%) site. Mineral dust as a source of WSON has been well-established in the Eastern Mediterranean (Violaki et al., 2010), with Nehir and Koçak (2018) attributing 10% of PM_{10} WSON to crustal material. Transported dust can also act as a platform to convey ON compounds from distant areas (Shi et al., 2010). Yu et al. (2017) reported variable contributions of dust to WSON in $PM_{2.5}$, in the Pearl River Delta, ranging between 9 and 29%, while a 24% contribution of fugitive dust was found in Beijing by Liu et al. (2019).

K-rich aerosol: The factor, dominated by water-soluble potassium (thus, characterized as K-rich) and to a lesser extent by OC and EC, can be cautiously attributed to biomass burning. Biomass burning has been shown to be a potent contributor to urban fine particles in Cyprus, accounting for 14–20% of $PM_{2.5}$ on an annual basis (Achilleos et al., 2016). The average contribution of the factor at NIC-TRA during winter was by 41% higher ($p = 0.06$) compared to the rest of the year, indicating a possible input of biomass burning for heating purposes. This was not observed at the regional background site, which could be comparatively more affected by regionally transported plumes. Contributions at EMEP were enhanced during July–August and peaked in early September (Fig. S6), consistent with findings from multi-year observations in the Eastern Mediterranean, regarding the transport of emissions from agricultural waste burning in the Black Sea region (Sciare et al., 2008). Indeed, air mass trajectories from the northern sectors were associated with 68% higher contributions at EMEP, on average. The lack of an inter-site correlation ($r = 0.25$) between the contributions of the factor probably suggests local contribution of domestic heating during winter in Nicosia. The CPF plot of K-rich source contributions at NIC-TRA (Fig. S7) further indicates the locality of the source, possibly related to BB emissions in the area of Nicosia. The K-rich factor contributed about 16% of WSON at both sites. The emission of numerous ON compounds, including nitro-phenols, amides and N-heterocyclic compounds, from biomass burning has been documented experimentally (Simoneit et al., 2002; Iinuma et al., 2007) and the importance of the source has emerged by most of the relevant field studies. Large, location-dependent, contributions of biomass burning to WSON in $PM_{2.5}$ (8–51%) were reported in South China by Yu et al. (2017), while Liu et al. (2019) in Beijing estimated a mean contribution of about 8%. Chen et al. (2010) also presented a PMF-resolved biomass-burning factor in Taiwan.

Vehicular emissions (at the roadside site): At NIC-TRA, the factor associated with vehicular emissions contributed significantly to WSON concentrations (35%). The source profile is characterized by high loadings on OC and EC, which are found in tailpipe emissions, as well as on Cu and Zn originating from automotive wear (brakes, tires) [Lough et al., 2005; Grivas et al., 2018]. The OC/EC ratio in the factor was 1.6, which is reasonable for direct emissions from the mainly gasoline-powered fleet in Cyprus. The factor correlated well with traffic-related gaseous pollutants ($r = 0.63$ and 0.72 with NO_2 and CO, respectively). The local character of the vehicular source is also indicated by the CPF plot in Fig. S7, with maximum contributions being associated with low-wind conditions, indicating the stagnation effect for freshly produced emissions from traffic (Masiol et al., 2017). In accordance to the variation of urban emissions in Nicosia (Fig. 4), the mean contribution of this source decreased markedly (54% lower, $p < 0.01$) during the summer period (Fig. S6). Vehicular emissions accounted for 35% of WSON concentrations, an important contribution, close to the mean vehicular contribution to $PM_{2.5}$ WSON (45%) reported by Yu et al. (2017) for a roadside site in Guangzhou. The respective contribution presented by Chen et al. (2019) in Beijing was smaller (13%), however,

when sampling at a height of 30 m. Regarding the potential composition of traffic-derived WSON, particle-bound amines have been recognized as an important component of traffic emissions, with their contribution even accounting for a respectable fraction of total organic mass (Gilardoni et al., 2009). Perrone et al. (2016) reported considerable amounts of alkylamines (ca. 50 ng m^{-3}) in particles sampled at traffic sites in Milan, Italy. The presence of amine-rich particles in vehicular emissions has also been assessed by laboratory studies (Sodeman et al., 2005; Toner et al., 2006).

Fossil fuel combustion (at the background site): The remaining factor identified at the background site had a very low contribution to WSON (6%). It is characterized by increased loadings in EC and OC and to a lesser extent to elements contained in emissions from oil combustion (mainly Pb). The factor was uncorrelated ($r = 0.14$) with the vehicular source identified at Nicosia. Consequently, it is very unlikely to be related to urban vehicular emissions directly transported to the site. It was also differentiated from the regional secondary source by an absence of sulfate, by a relative absence of seasonality and air mass history dependence, and by a lower OC/EC ratio (4.3 compared to 9.5) indicating a smaller degree of atmospheric processing. The factor should be attributed to fossil fuel combustion emissions in the general vicinity of the site, as indicated by the significant correlation with SO_2 ($r = 0.43$). As a result, transport from point sources should also be considered in this factor, such as from the oil-fired power plants to the south-east of the site. Such local transport has been documented by Debevec et al. (2017) for anthropogenic VOCs at the same site and by Achilleos et al. (2016) for PM at multiple locations in Cyprus. In fact, the CPF plot (Fig. S7) indicates a larger probability of high contributions for strong winds from the E-SE of the site, an axis for which transport processes across Cyprus have been documented (Kleanthous et al., 2014). In general, the emission of WSON from oil combustion has received little attention, with Yu et al. (2017) recently reporting important contributions of heavy oil combustion to WSON in the Pearl River Delta area (in the range of 8–12%).

4. Conclusions

This study presents one of the first attempts to study the factors controlling the variability and sources of water-soluble organic nitrogen (WSON) at contrasted locations in the Eastern Mediterranean, on both spatial and temporal scales, for a time-extended (1-year) period. Atmospheric sampling at monitoring sites of completely different typology (urban traffic vs. rural background) allowed for a direct estimation of the contribution of local anthropogenic emissions. While a clear urban/traffic influence was evidenced by both the examination of temporal variation and the source apportionment, the overall inter-site difference in WSON concentrations was a mere 25% on an annual basis (9% if only the concurrent samples were considered). Similar urban against regional background patterns have been found for WSON in large metropolitan areas around the world, emphasizing the importance of transport and secondary processing mechanisms on both regional and local scales. Considering the identified controlling factors - that include air mass history, meteorology, atmospheric chemistry, and both anthropogenic and natural emissions - it appears that WSON shares the complexity of fine particles and organic aerosol in terms of source multiplicity and secondary influences. The participation of WSON to total soluble nitrogen was around 20% on average, with limited inter-site and seasonal variability and also being comparable with global model estimations for soluble ON/TN in deposition over the Eastern Mediterranean (Kanakidou et al., 2012). The “Lenschow approach” revealed almost equivalent “urban + traffic” and regional contributions to WSON during the cold period, confirming the importance of traffic emissions, while the contributions of regional aerosols became more important during summer.

The source apportionment study identified that regional secondary contributions (long-range transport, atmospheric processing) accounted annually for about 60% and 40% of WSON at the regional background and urban sites, respectively, with a significant inter-site correlation. At the same time, a vehicular contribution exceeding 30% was found at the roadside location. Natural primary sources had small contributions, with mineral dust impacts being limited during the year of measurements (<10%) and marine aerosols having a very weak signal (2–3%). However, the lack of specific aerosol tracers for biogenic emissions did not allow the PMF models to account for the variability of additional natural ON sources (e.g primary biogenic). Detailed and size-resolved chemical speciation of WSON and availability of additional organic tracers, utilized in a PMF framework, can improve WSON source characterization. Meanwhile, the evolution of advanced aerosol mass spectrometric techniques for the characterization of the numerous ON groups and compounds (Altieri et al., 2009) appears very promising, as it can also lead to source apportionment with sub-daily resolution, which is an important scale of variability for the assessment of rapid chemical processes. Until these methods become more accessible, additional filter-based receptor modeling studies in different settings would be rather useful to further our understanding of WSON sources and their relative contributions.

CRediT authorship contribution statement

Maria Tsagkaraki: Methodology, Investigation, Data curation, Writing - review & editing. **Christina Theodosi:** Methodology, Investigation, Data curation. **Georgios Grivas:** Writing - original draft, Formal analysis, Methodology, Investigation, Data curation. **Evanthia Vargiakaki:** Methodology, Investigation, Data curation. **Jean Sciare:** Writing - review & editing, Funding acquisition. **Chrysanthos Savvides:** Writing - review & editing, Resources. **Nikolaos Mihalopoulos:** Conceptualization, Writing - review & editing, Funding acquisition, Supervision.

Declaration of competing interest

The authors declare that they have no known competing financial interests or personal relationships that could have appeared to influence the work reported in this paper.

Acknowledgements

The authors would like to thank Emily Vasiliadou and Christos Kizas from the Department of Labour Inspection (DLI), Ministry of Labour, Welfare and Social Insurance, for providing filters, air quality and meteorological parameters from EMEP and NIC-TRA sites. This study has received support from the AQ-SERVE project (Air Quality Services for a cleaner air in Cyprus (INTEGRATED/0916/0016) funded by the Cyprus Research and Innovation Foundation. The article is dedicated to the memory of Savvas Kleanthous, former Head of Air Quality Section of the Department of Labour Inspection.

Appendix A. Supplementary data

Supplementary data to this article can be found online at https://doi.org/10.1016/j.atmosenv.2020.118144.

References

Achilleos, S., Evans, J.S., Yiallouros, P.K., Kleanthous, S., Schwartz, J., Koutrakis, P., 2014. PM_{10} concentration levels at an urban and background site in Cyprus: the impact of urban sources and dust storms. J. Air Waste Manag. Assoc. 64, 1352–1360.

Achilleos, S., Wolfson, J.M., Ferguson, S.T., Kang, C.M., Hadjimitsis, D.G., Hadjicharalambous, M., Achilleos, C., Christodoulou, A., Nisanzti, A., Papoutsa, C., Themistocleous, K., Athanasatos, S., Perdikou, S., Koutrakis, P., 2016. Spatial variability of fine and coarse particle composition and sources in Cyprus. Atmos. Res. 169, 255–270.

Altieri, K., Turpin, B.J., Seitzinger, S.P., 2009. Composition of dissolved organic nitrogen in continental precipitation investigated by ultra-high resolution FT-ICR mass spectrometry. Environ. Sci. Technol. 43, 6950–6955.

Altieri, K., Fawcett, S., Peters, A., Sigman, D., Hastings, M., 2016. Marine biogenic source of atmospheric organic nitrogen in the subtropical North Atlantic. Proc. Nat. Acad. Sci. USA 113, 925–930.
Bardouki, H., Liakakou, H., Economou, C., Sciare, J., Smolík, J., Ždímal, V., Eleftheriadis, K., Lazaridis, M., Dye, C., Mihalopoulos, N., 2003. Chemical composition of size-resolved atmospheric aerosols in the eastern Mediterranean during summer and winter. Atmos. Environ. 37, 195–208.
Booyens, W., Van Zyl, P.G., Beukes, J.P., Ruiz-Jimenez, J., Kopperi, M., Riekkola, M.-L., Vakkari, V., Josipovic, M., Kulmala, M., Laakso, L., 2019. Characterising particulate organic nitrogen at a savannah-grassland region in South Africa. Atmosphere 10, 492.
Briggs, Nicole, Long, L., Christopher, M., 2016. Critical review of black carbon and elemental carbon source apportionment in Europe and the United States. Atmos. Environ. 144, 409–427.
Brown, S.G., Eberly, S., Paatero, P., Norris, G.A., 2015. Methods for estimating uncertainty in PMF solutions: examples with ambient air and water quality data and guidance on reporting PMF results. Sci. Total Environ. 518–519, 626–635.
Cape, J.N., Cornell, S.E., Jickells, T.D., Nemitz, E., 2011. Organic nitrogen in the atmosphere - where does it come from? A review of sources and methods. Atmos. Res. 102, 30–48.
Cavalli, F., Viana, M., Yttri, K.E., Genberg, J., Putaud, J.-P., 2010. Toward a standardised thermal-optical protocol for measuring atmospheric organic and elemental carbon: the EUSAAR protocol. Atmos. Meas. Techn. 3, 79–89.
Chen, H.Y., Chen, L.D., 2010. Occurrence of water soluble organic nitrogen in aerosols at a coastal area. J. Atmos. Chem. 65, 49–71.
Chen, H.Y., Chen, L.D., Chiang, Z.Y., Hung, C.C., Lin, F.J., Chou, W.C., Gong, G.C., Wen, L.S., 2010. Size fractionation and molecular composition of water-soluble inorganic and organic nitrogen in aerosols of a coastal environment. J. Geophys. Res. 115, D22307.
Chen, X., Xie, M., Hays, M.D., Edgerton, E., Schwede, D., Walker, J.T., 2018. Characterization of organic nitrogen in aerosols at a forest site in the southern Appalachian Mountains. Atmos. Chem. Phys. 18, 6829–6846.
Chen, Y., Chen, Y., Xie, X., Ye, Z., Li, Q., Ge, X., Chen, M., 2019. Chemical characteristics of $PM_{2.5}$ and water-soluble organic nitrogen in Yangzhou, China. Atmosphere 10, 178.
Comero, S., Capitani, L., Gawlik, B.M., 2009. Positive Matrix Factorisation (PMF). Environmental Monitoring Data Using PMF. JRC Scientific and Technical Reports, EUR 23946 EN.
Cornell, S.E., 2011. Atmospheric nitrogen deposition: revisiting the question of the importance of the organic component. Environ. Pollut. 159, 2214–2222.
Cornell, S., Mace, K., Coeppicus, S., Duce, R., Huebert, B., Jickells, T., Zhuang, L.-Z., 2001. Organic nitrogen in Hawaiian rain and aerosol. J. Geophys. Res. 106 (D8), 7973–7983.
Cornell, S.E., Jickells, T.D., Cape, J.N., Rowland, A.P., Duce, R.A., 2003. Organic nitrogen deposition on land and coastal environments: a review of methods and data. Atmos. Environ. 37, 2173–2191.
Debevec, C., Sauvage, S., Gros, V., Sciare, J., Pikridas, M., Stavroulas, I., Salameh, T., Leonardis, T., Gaudion, V., Depelchin, L., Fronval, I., Sarda-Esteve, R., Baisnée, D., Bonsang, B., Savvides, C., Vrekoussis, M., Locoge, N., 2017. Origin and variability in volatile organic compounds observed at an Eastern Mediterranean background site (Cyprus). Atmos. Chem. Phys. 17, 11355–11388, 2017.
Debevec, C., Sauvage, S., Gros, V., Sellegri, K., Sciare, J., Pikridas, M., Stavroulas, I., Leonardis, T., Gaudion, V., Depelchin, L., Fronval, I., Sarda-Esteve, R., Baisnée, D., Bonsang, B., Savvides, C., Vrekoussis, M., Locoge, N., 2018. Driving parameters of biogenic volatile organic compounds and consequences on new particle formation observed at an eastern Mediterranean background site. Atmos. Chem. Phys. 18, 14297–14325, 2018.
Duan, F., Liu, X., He, K., Dong, S., 2009. Measurements and characteristics of nitrogen-containing compounds in atmospheric particulate matter in Beijing, China. Bull. Environ. Contam. Toxicol. 82, 332–337.
Duce, R.A., Liss, P.S., Merrill, J.T., Atlas, E.L., Buat-Menard, P., Hicks, B.B., Miller, J.M., Prospero, J.M., Arimoto, R., Church, T.M., Ellis, W., Galloway, J.N., Hansen, L., Jickells, T.D., Knap, A.H., Reinhardt, K.H., Schneider, B., Soudine, A., Tokos, J.J., Tsunogai, S., Wollast, R., Zhou, M., 1991. The atmospheric input of trace species to the world ocean. Global Biogeochem. Cycles 5, 193–259.
Ervens, B., Turpin, B.J., Weber, R.J., 2011. Secondary organic aerosol formation in cloud droplets and aqueous particles (aqSOA): a review of laboratory, field and model studies. Atmos. Chem. Phys. 11, 11069–11102.
Facchini, M.C., Decesari, S., Rinaldi, M., Carbone, C., Finessi, E., Mircea, M., Fuzzi, S., Moretti, F., Tagliavini, E., Ceburnis, D., O'Dowd, C.D., 2008. Important source of marine secondary organic aerosol from biogenic amines. Environ. Sci. Technol. 42, 9116–9121.
Fowler, D., Steadman, C.E., Stevenson, D., Coyle, M., Rees, R.M., Skiba, U.M., Sutton, M. A., Cape, J.N., Dore, A.J., Vieno, M., Simpson, D., Zaehle, S., Stocker, B.D., Rinaldi, M., Facchini, M.C., Flechard, C.R., Nemitz, E., Twigg, M., Erisman, J.W., Butterbach-Bahl, K., Galloway, J.N., 2015. Effects of global change during the 21st century on the nitrogen cycle. Atmos. Chem. Phys. 15, 13849–13893.
Galloway, J.N., Aber, J.D., Erisman, J.W., Seitzinger, S.P., Howarth, R.W., Cowling, E.B., Cosby, B.J., 2003. The nitrogen cascade. Bioscience 53, 341–356.
Georgiou, G.K., Kushta, J., Christoudias, T., Proestos, Y., Lelieveld, J., 2020. Air quality modeling over the Eastern Mediterranean: seasonal sensitivity to anthropogenic emissions. Atmos. Environ. 222, 117119.
Gilardoni, S., Liu, S., Takahama, S., Russell, L.M., Allan, J.D., Steinbrecher, R., Jimenez, J.L., De Carlo, P.F., Dunlea, E.J., Baumgardner, D., 2009. Characterization of organic ambient aerosol during MIRAGE 2006 on three platforms. Atmos. Chem. Phys. 9, 5417–5432.
Grivas, G., Cheristanidis, S., Chaloulakou, A., Koutrakis, P., Mihalopoulos, N., 2018. Elemental composition and source apportionment of fine and coarse particles at traffic and urban background locations in Athens, Greece. Aerosol. Air Qual. Res. 18, 1642–1659.
Guerzoni, S., Chester, R., Dulac, F., Herut, B., Loÿe-Pilot, M.-D., Measures, C., Migon, C., Molinaroli, E., Moulin, C., Rossini, P., Saydam, C., Soudine, A., Ziveri, P., 1999. The role of atmospheric deposition in the biogeochemistry of the Mediterranean Sea. Prog. Oceanogr. 44, 147–190.
Harrison, M.A.J., Barra, S., Borghesi, D., Vione, D., Arsene, C., Iulian Olariu, R., 2005. Nitrated phenols in the atmosphere: a review. Atmos. Environ. 39, 231–248.
Hasheminassab, S., Daher, N., Ostro, B.D., Sioutas, C., 2014. Long-term source apportionment of ambient fine particulate matter ($PM_{2.5}$) in the Los Angeles Basin: a focus on emissions reduction from vehicular sources. Environ. Pollut. 193, 54–64.
Ho, K.F., Ho, S.S.H., Huang, R.-J., Liu, S.X., Cao, J.-J., Zhang, T., Chuang, H.-C., Chan, C. S., Hu, D., Tian, L., 2015. Characteristics of water-soluble organic nitrogen in fine particulate matter in the continental area of China. Atmos. Environ. 106, 252–261.
Iinuma, Y., Brüggemann, E., Gnauk, T., Müller, K., Andreae, M.O., Helas, G., Parmar, R., Herrmann, H., 2007. Source characterization of biomass burning particles: the combustion of selected European conifers, African hardwood, savanna grass, and German and Indonesian peat. J. Geophys. Res. 112, D08209.
Jickells, T., Baker, A.R., Cape, J.N., Cornell, S.E., Nemitz, E., 2013. The cycling of organic nitrogen through the atmosphere. Phil. Trans. Roy. Soc. Lond. B 368, 20130115.
Kanakidou, M., Duce, R.A., Prospero, J.M., Baker, A.R., Benitez-Nelson, C., Dentener, F. J., Hunter, K.A., Liss, P.S., Mahowald, N., Okin, G.S., Sarin, M., Tsigaridis, K., Uematsu, M., Zamora, L.M., Zhu, T., 2012. Atmospheric fluxes of organic N and P to the global ocean. Global Biogeochem. Cycles 26, GB3026.
Kanakidou, M., Myriokefalitakis, S., Tsagkaraki, M., 2020. Atmospheric inputs of nutrients to the mediterranean sea. Deep-Sea Res. Part II Top. Stud. Oceanogr. 171, 104606.
Kaskaoutis, D.G., Grivas, G., Theodosi, C., Tsagkaraki, M., Paraskevopoulou, D., Stavroulas, I., Liakakou, E., Gkikas, A., Hatzianastassiou, N., Wu, C., Gerasopoulos, E., Mihalopoulos, N., 2020. Carbonaceous aerosols in contrasting atmospheric environments in Greek Cities: evaluation of the EC-tracer methods for secondary organic carbon estimation. Atmosphere 11, 161.
Kleanthous, S., Vrekoussis, M., Mihalopoulos, N., Kalabokas, P., Lelieveld, J., 2014. On the temporal and spatial variation of ozone in Cyprus. Sci. Total Environ. 476–477, 677–687.
Kouvarakis, G., Tsigaridis, K., Kanakidou, M., Mihalopoulos, N., 2000. Temporal variations of surface regional background ozone over Crete Island in the southeast Mediterranean. J. Geophys. Res. 105 (D4), 4399–4407.
Krom, M.D., Herut, B., Mantoura, R.F.C., 2004. Nutrient budget for the eastern mediterranean: implications for phosphorus limitation. Limnol. Oceanogr. 49, 1582–1592.
Lelieveld, J., Berresheim, H., Borrmann, S., Crutzen, P.J., Dentener, F.J., Fischer, H., Feichter, J., Flatau, P.J., Heland, J., Holzinger, R., Korrmann, R., Lawrence, M.G., Levin, Z., Markowicz, K.M., Mihalopoulos, N., Minikin, A., Ramanathan, V., De Reus, M., Roelofs, G.J., Scheeren, H.A., Sciare, J., Schlager, H., Schultz, M., Siegmund, P., Steil, B., Stephanou, E.G., Stier, P., Traub, M., Warneke, C., Williams, J., Ziereis, H., 2002. Global air pollution crossroads over the Mediterranean. Science 298, 794–799.
Lenschow, P., Abraham, H.J., Kutzner, K., Lutz, M., Preuss, J.D., Reichenbächer, W., 2001. Some ideas about the sources of PM_{10}. Atmos. Environ. 35, 123–133.
Li, X., Hede, T., Tu, Y., Leck, C., Gren, H.A., 2013. Cloud droplet activation mechanisms of amino acid aerosol particles: Insight from molecular dynamics simulations, Tellus. Ser. B: Chem. Phys. Meteorol. 65, 20476.
Liu, Q., Baumgartner, J., Schauer, J.J., 2019. Source Apportionment of fine-particle, water-soluble organic nitrogen and its association with the inflammatory potential of lung epithelial cells. Environ. Sci. Technol. 53, 9845–9854.
Lough, G.C., Schauer, J.J., Park, J.S., Shafer, M.M., DeMinter, J.T., Weinstein, J.P., 2005. Emissions of metals associated with motor vehicle roadways. Environ. Sci. Technol. 39, 826–836.
Mace, K.A., Artaxo, P., Duce, R.A., 2003a. Water-soluble organic nitrogen in Amazon Basin aerosols during the dry (biomass burning) and wet seasons. J. Geophys. Res. 108 (D16), 4512.
Mace, K.A., Kubilay, N., Duce, R.A., 2003b. Organic nitrogen in rain and aerosol in the eastern Mediterranean atmosphere: An association with atmospheric dust. J. Geophys.Res. 108 (D10), 4320.
Maheras, P., Flocas, H.A., Patrikas, I., Anagnostopoulou, C.H.R., 2004. A 40 year objective climatology of surface cyclones in the mediterranean region: spatial and temporal distribution. Int. J. Climatol. 21, 109–130.
Markaki, Z., Loÿe-Pilot, M.D., Violaki, K., Benyahya, L., Mihalopoulos, N., 2010. Variability of atmospheric deposition of dissolved nitrogen and phosphorus in the Mediterranean and possible link to the anomalous seawater N/P ratio. Mar. Chem. 120, 187–194.
Masiol, M., Hopke, P.K., Felton, H.D., Frank, B.P., Rattigan, O.V., Wurth, M.J., LaDuke, G.H., 2017. Analysis of major air pollutants and submicron particles in New York City and Long Island. Atmos. Environ. 148, 203–214.
Matsumoto, K., Yamamoto, Y., Kobayashi, H., Kaneyasu, N., Nakano, T., 2014. Water-soluble organic nitrogen in the ambient aerosols and its contribution to the dry deposition of fixed nitrogen species in Japan. Atmos. Environ. 95, 334–343.
Matsumoto, K., Takusagawa, F., Suzuki, H., Horiuchi, K., 2018. Water-soluble organic nitrogen in the aerosols and rainwater at an urban site in Japan: implications for the nitrogen composition in the atmospheric deposition. Atmos. Environ. 191, 267–272.
Middleton, N., Yiallouros, P., Kleanthous, S., Kolokotroni, O., Schwartz, J., Dockery, D. W., Demokritou, P., Koutrakis, P., 2008. A 10-year time-series analysis of respiratory

and cardiovascular morbidity in Nicosia, Cyprus: the effect of short-term changes in air pollution and dust storms. Environ. Health 7, 39.
Miyazaki, Y., Kawamura, K., Jung, J., Furutani, H., Uematsu, M., 2011. Latitudinal distributions of organic nitrogen and organic carbon in marine aerosols over the western North Pacific. Atmos. Chem. Phys. 11, 3037–3049.
Miyazaki, Y., Fu, P.Q., Ono, K., Tachibana, E., Kawamura, K., 2014. Seasonal cycles of water-soluble organic nitrogen aerosols in a deciduous broadleaf forest in northern Japan. J. Geophys. Res. Atmos. 119, 1440–1454.
Montero-Martínez, G., Rinaldi, M., Gilardoni, S., Giulianelli, L., Paglione, M., Decesari, S., Fuzzi, S., Facchini, M.C., 2014. On the water-soluble organic nitrogen concentration and mass size distribution during the fog season in the Po Valley, Italy. Sci. Total Environ. 485–486, 103–109.
Mouzourides, P., Kumar, P., Neophytou, M.K.-A., 2015. Assessment of long-term measurements of particulate matter and gaseous pollutants in South-East Mediterranean. Atmos. Environ. 107, 148–165.
Nehir, M., Koçak, M., 2017. Atmospheric water-soluble organic nitrogen (WSON) in the eastern Mediterranean: origin and ramifications regarding marine productivity. Atmos. Chem. Phys. 18, 3603–3618.
Norris, G., Vedantham, R., Wade, K., Brown, S., Pouty, J., Foley, C., Martin, L., 2008. EPA Positive Matrix Factorization (PMF) 3.0 Fundamentals & User Guide. United States Environmental Protection Agency. EPA 600/R-08/108.
Norris, G., Duvall, R., Brown, S., Bai, S., 2014. EPA Positive Matrix Factorization (PMF) 5.0 Fundamentals and User Guide. EPA PMF 5. 0 Fundamentals and User Guide. United States Environmental Protection Agency. EPA/600/R-14/108.
Özel, M.Z., Hamilton, J.F., Lewis, A.C., 2010. New sensitive and quantitative analysis method for organic nitrogen compounds in urban aerosol samples. Environ. Sci. Technol. 45, 1497–1505.
Paatero, P., 1999. The multilinear engine-a table-driven least squares program for solving multilinear problems, including the n-way parallel factor analysis model. J. Comput. Graph Stat. 8, 854–888.
Paatero, P., Hopke, P.K., 2003. Discarding or downweighting high-noise variables in factor analytic models. Anal. Chim. Acta 490, 277–289.
Paatero, P., Hopke, P.K., Song, X.-H., Ramadan, Z., 2002. Understanding and controlling rotations in factor analytic models. Chemometr. Intell. Lab. Syst. 60, 253–264.
Paatero, P., Eberly, S.I., Brown, S.G., Norris, G.A., 2014. Methods for estimating uncertainty in factor analytic solutions. Atmos. Meas. Techn. 7, 781–797.
Paraskevopoulou, D., Liakakou, E., Gerasopoulos, E., Theodosi, C., Mihalopoulos, N., 2014. Long-term characterization of organic and elemental carbon in the $PM_{2.5}$ fraction: the case of Athens, Greece. Atmos. Chem. Phys. 14, 13313–13325.
Pashardes, S., Christofides, C., 1995. Statistical analysis of wind speed and direction in Cyprus. Sol. Energy 55, 405–414.
Perrone, M.G., Zhou, J., Malandrino, M., Sangiorgi, G., Rizzi, C., Ferrero, L., Dommen, J., Bolzacchini, 2016. PM chemical composition and oxidative potential of the soluble fraction of particles at two sites in the urban area of Milan, Northern Italy. Atmos. Environ. 128, 104–113.
Pikridas, M., Vrekoussis, M., Sciare, J., Kleanthous, S., Vasiliadou, E., Kizas, C., Savvides, C., Mihalopoulos, N., 2018. Spatial and temporal (short and long-term) variability of submicron, fine and sub-10 μm particulate matter (PM_1, $PM_{2.5}$, PM_{10}) in Cyprus. Atmos. Environ. 191, 79–93.
Polissar, A.V., Hopke, P.K., Paatero, P., Malm, W.C., Sisler, J.F., 1998. Atmospheric aerosol over Alaska 2. Elemental composition and sources. J. Geophys. Res. 103 (D15), 19045–19057.
Qiu, C., Zhang, R., 2012. Physiochemical properties of alkylaminium sulfates: hygroscopicity, thermostability, and density. Environ. Sci. Technol. 46, 4474–4480.
Rastogi, N., Zhang, X., Edgerton, E.S., Ingall, E., Weber, R.J., 2011. Filterable water-soluble organic nitrogen in fine particles over the southeastern USA during summer. Atmos. Environ. 45, 6040–6047.
Reff, A., Eberly, S.I., Bhave, P.V., 2007. Receptor modeling of ambient particulate matter data using positive matrix factorization: review of existing methods. J. Air Waste Manag. Assoc. 57, 146–154.
Russell, A.G., McRae, G.J., Cass, G.R., 1983. Mathematical modeling of the formation and transport of ammonium nitrate aerosol. Atmos. Environ. 17, 949–964.
Sciare, J., Oikonomou, K., Favez, O., Liakakou, E., Markaki, Z., Cachier, H., Mihalopoulos, N., 2008. Long-term measurements of carbonaceous aerosols in the Eastern Mediterranean: evidence of long-range transport of biomass burning. Atmos. Chem. Phys. 8, 5551–5563.
Simoneit, B.R.T., Rushdi, A.I., bin Abas, M.R., Didyk, B.M., 2002. Alkyl amides and nitriles as novel tracers for biomass burning. Environ. Sci. Technol. 37, 16–21.
Sodeman, D.A., Toner, S.M., Prather, K.A., 2005. Determination of single particle mass spectral signatures from light-duty vehicle emissions. Environ. Sci. Technol. 39, 4569–4580.
Srivastava, D., Favez, O., Perraudin, E., Villenave, E., Albinet, A., 2018. Comparison of measurement-based methodologies to apportion secondary organic carbon (SOC) in $PM_{2.5}$: a review of recent studies. Atmosphere 9, 452.
Stavroulas, I., Bougiatioti, A., Grivas, G., Paraskevopoulou, D., Tsagkaraki, M., Zarmpas, P., Liakakou, E., Gerasopoulos, E., Mihalopoulos, N., 2019. Sources and processes that control the submicron organic aerosol composition in an urban Mediterranean environment (Athens): a high temporal-resolution chemical composition measurement study. Atmos. Chem. Phys. 19, 901–919.
Theodosi, C., Markaki, Z., Tselepides, A., Mihalopoulos, N., 2010. The significance of atmospheric inputs of soluble and particulate major and trace metals to the Eastern Mediterranean Sea,. Mar. Chem. 120, 154–163.
Theodosi, C., Tsagkaraki, M., Zarmpas, P., Grivas, G., Liakakou, E., Paraskevopoulou, D., Lianou, M., Gerasopoulos, E., Mihalopoulos, N., 2018. Multi-year chemical composition of the fine-aerosol fraction in Athens, Greece, with emphasis on the contribution of residential heating in wintertime. Atmos. Chem. Phys. 18, 14371–14391.
Toner, S.M., Sodeman, D.A., Prather, K.A., 2006. Single particle characterization of ultrafine and accumulation mode particles from heavy duty diesel vehicles using aerosol time-of-flight mass spectrometry. Environ. Sci. Technol. 40, 3912–3921.
Turpin, B.J., Huntzicker, J.J., 1995. Identification of secondary organic aerosol episodes and quantification of primary and secondary organic aerosol concentrations during SCAQS. Atmos. Environ. 23, 3527–3544.
Uria-Tellaetxe, I., Carslaw, D.C., 2014. Conditional bivariate probability function for source identification. Environ. Model. Software 59, 1–9.
Violaki, K., Mihalopoulos, N., 2010. Water-soluble organic nitrogen (WSON) in size-segregated atmospheric particles over the Eastern Mediterranean. Atmos. Environ. 44, 4339–4345.
Violaki, K., Zarbas, P., Mihalopoulos, N., 2010. Long-term measurements of dissolved organic nitrogen (DON) in atmospheric deposition in the Eastern Mediterranean: fluxes, origin and biogeochemical implications. Mar. Chem. 120, 179–186.
Violaki, K., Sciare, J., Williams, J., Baker, A.R., Martino, M., Mihalopoulos, N., 2015. Atmospheric water-soluble organic nitrogen (WSON) over marine environments: a global perspective. Biogeosciences 12, 3131–3140.
Wang, G.H., Zhou, B.H., Cheng, C.L., Cao, J.J., Li, J.J., Meng, J.J., Tao, J., Zhang, R.J., Fu, P.Q., 2013. Impact of Gobi desert dust on aerosol chemistry of Xi'an, inland China during spring 2009: differences in composition and size distribution between the urban ground surface and the mountain atmosphere. Atmos. Chem. Phys. 13, 819–835.
Ye, Z., Li, Q., Ma, S., Zhou, Q., Gu, Y., Su, Y., Chen, Y., Chen, H., Wang, J., Ge, X., 2017. Summertime day-night differences of $PM_{2.5}$ components (inorganic ions, OC, EC, WSOC, WSON, HULIS, and PAHs) in changzhou, China. Atmosphere 8, 189.
Yu, X., Yu, Q., Zhu, M., Tang, M., Li, S., Yang, W., Zhang, Y., Deng, W., Li, G., Yu, Y., Huang, Z., Song, W., Ding, X., Hu, Q., Li, J., Bi, X., Wang, X., 2017. Water soluble organic nitrogen (WSON) in ambient fine particles over a megacity in South China: spatiotemporal variations and source apportionment. J. Geophys. Res.: Atmos. 122, 13045–13060.